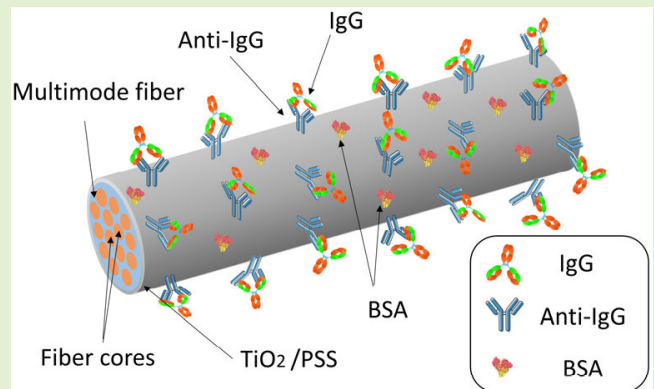


# Direct Functionalization of TiO<sub>2</sub>/PSS Sensing Layer for an LMR-Based Optical Fiber Reusable Biosensor

Desiree Santano Rivero<sup>ID</sup>, Abián B. Socorro-Leránz<sup>ID</sup>, and Ignacio Del Villar<sup>ID</sup>, *Member, IEEE*

**Abstract**—Functionalization plays a crucial role in the development of biosensors. In this study, bioreceptors were directly immobilized onto the surface of a sensing layer after physical activation, avoiding the need for longer and more complex functionalization systems. This direct immobilization was applied to an optical sensing platform based on lossy mode resonances (LMRs) generated by a thin film of titanium (IV) dioxide/poly(sodium 4-styrenesulfonate) (TiO<sub>2</sub>/PSS). To generate the LMR, a 200- $\mu\text{m}$  bare optical fiber was coated with TiO<sub>2</sub>/PSS using the layer-by-layer self-assembly technique. The PSS of the sensing layer was then physically activated using either UV-ozone or plasma to immobilize antirabbit immunoglobulin G (IgG) bioreceptors. This enabled specific and label-free detection of rabbit IgG concentrations ranging from 0.002 to 2 mg/mL. The results presented in this work include the real-time detection of rabbit IgG, a comparison between the two activation techniques (UV-ozone and plasma), and an analysis of the biosensor's reusability over four consecutive cycles, which demonstrates the promising potential of the TiO<sub>2</sub>/PSS sensing layer for biosensing applications.



**Index Terms**—Biosensor, layer-by-layer (LbL), lossy mode resonance (LMR), optical fiber, titanium (IV) dioxide (TiO<sub>2</sub>) thin film.

## I. INTRODUCTION

OPTICAL fiber sensing is a technology that has experienced much progress thanks to decades of research, especially in the domain of chemical sensors and biosensors

Manuscript received 21 August 2023; revised 10 October 2023; accepted 17 October 2023. Date of publication 6 November 2023; date of current version 14 December 2023. This work was supported in part by the Spanish Agencia Estatal de Investigación (AEI) under Grant PID2019-106231RB-I00, in part by the Public University of Navarra under Grant PJUPNA2033, and in part by the Ph.D. Grant by the Public University of Navarra. The associate editor coordinating the review of this article and approving it for publication was Dr. Minghong Yang. (Corresponding author: Desiree Santano Rivero.)

Desiree Santano Rivero is with the IEEC Department, Public University of Navarra, 31006 Pamplona, Spain (e-mail: desiree.santano@unavarra.es).

Abián B. Socorro-Leránz is with the Department of Electrical, Electronic and Communication Engineering and the Institute of Smart Cities (ISC), Public University of Navarra, 31006 Pamplona, Spain, and also with the Navarra Institute for Health Research (IdiSNA), Recinto del Hospital Universitario de Navarra, E-31008 Pamplona, Spain (e-mail: ab.socorro@unavarra.es).

Ignacio Del Villar is with the Department of Electrical, Electronic and Communication Engineering and the Institute of Smart Cities (ISC), Public University of Navarra, 31006 Pamplona, Spain (e-mail: ignacio.delvillar@unavarra.es).

This article has supplementary downloadable material available at <https://doi.org/10.1109/JSEN.2023.3328810>, provided by the authors.

Digital Object Identifier 10.1109/JSEN.2023.3328810

[1], [2]. This is possible because it is cost-effective and biocompatible [3] and because the optical fiber is flexible and small in size and weight [4], which allows monitoring physical variables within the organism with a catheter [5], for instance. Moreover, fiber optics has demonstrated the ability to perform measurements in hazardous environments such as nuclear facilities [6] and in strong magnetic fields due to its immunity to electromagnetic interference [2].

The deposition of thin films onto the sensitive area of the optical fiber leads to the generation of resonances whose spectral shift is employed to detect changes in either the thin film itself or in the subsequent deposition of additional layers [2]. In the generation of resonances, it is necessary to take into account the properties of the material used for the thin film. In the case of lossy mode resonances (LMRs), the real part of the material permittivity must be positive and higher in magnitude than both its own imaginary part and the real part of the permittivity of the material surrounding the thin film [7]. That is why LMRs are generated mainly with either metal oxides or polymer coatings [8], [9].

One of these materials is titanium (IV) dioxide (TiO<sub>2</sub>) [10], which has been widely used in biomedical applications due to its biocompatibility and corrosion resistance, making it an excellent choice for implants and prosthetics [11]. Moreover, the properties of TiO<sub>2</sub> make it a metal oxide with a promis-

ing future in biosensing applications. The influence of the surface properties of titanium on the biological response and the effect of different nanoscale surface modifications have been described previously [12]. Also, the photoelectrochemical biosensing field has been greatly benefited from the use of various TiO<sub>2</sub> nanostructures, including nanotubes and nanowires [13]. TiO<sub>2</sub> also offers physical and chemical resistance, which can extend the lifespan of a device. However, inducing a precise etching of TiO<sub>2</sub> thin films to achieve a particular profile is still a challenging task, especially on the nanoscale [14].

In the design and optimization of biosensors, the functionalization is a critical stage, as it ensures that the sensor can interact with the analyte and produce a detectable signal in response to its presence. The term “functionalization” refers to the process where the sensing surface is modified to allow the immobilization of the bioreceptors. Nowadays, several surface modification strategies are available in the literature. Choosing one of them depends on several aspects, such as the transducing mechanism of the sensor, the substrate, and the bioreceptor to be immobilized [16].

In this sense, direct physical adsorption is the simplest immobilization method, in which the biomolecules are directly attached to the surface through weak bonds such as van der Waals forces, hydrogen bonding, or hydrophobic interactions. Frequently, surface functionalization methods include self-assembled monolayers (SAMs), deposition of polymers, nanomaterials, and metal-organic frameworks (MOFs) to improve the efficiency and applicability of the sensors. There are different kinds of SAMs reported, which involve carboxylate SAMs on the oxide surfaces, silane SAMs on glass/silicon surfaces, and alkane thiol SAMs on noble metals [17].

Regarding optical fiber sensors, the focus of this work, it is well-described the subsequent activation of the previous mentioned thin films by means of crosslinkers, such as glutaraldehyde for silane SAMs [18], [19], [20] or N-ethyl-N'-(3-(dimethylamino) propyl) carbodiimide/N-hydroxysuccinimide (EDC/NHS) for alkane thiol SAMs and polymers [21], [22], [23], [24]. In the proposed biosensor, the generation of LMRs based on TiO<sub>2</sub> thin films is obtained by using the layer-by-layer (LbL) technique, including the presence of the polymer poly(sodium 4-styrenesulfonate) (PSS) in the sensing surface available for its direct activation, thus avoiding subsequent deposition steps, as it will be shown.

Additionally, surface modification techniques such as plasma or UV-ozone have been extensively used as a way to change the properties of the polymer surfaces. This treatment can activate chemically inactive groups that can be used in the functionalization of biosensors [25], [26], [27], [28]. This reduces significantly the number of steps and the time invested during the manufacturing process, as well as it guarantees the absence of any residual chemical solvents or contaminants [29].

Regarding bioreceptors, immunoglobulin G (IgG) is the most abundant human antibody and is regarded as a significant physiological indicator of the immune response. The detection of IgG allows wide-ranging applications in disease diagnosis, prognosis, and therapeutic monitoring [30]. Its measurement provides valuable insights to facilitate early detection and effective management of various infectious, autoimmune, and inflammatory diseases [31]. A traditional method for IgG detection is enzyme-linked immunosorbent assay (ELISA), which presents the disadvantages of labeled methods: high

cost, multistep processing, and long detection time [30]. Recently, various optical fiber biosensors have been developed for the detection of IgGs based on surface plasmon resonances (SPRs) [21], [22], [23], [32], [33], interferometers [18], [34], and Bragg gratings [20]. These strategies promote the development of label-free biosensors, leading the path to an actual and cost-effective alternative to the traditional clinical techniques.

In this article, the aim was to test and apply the physical activation techniques to optical fiber sensors as a time-effective functionalization method for the detection of biomolecules. To this purpose, a label-free LMR-based biosensing platform composed of a TiO<sub>2</sub>/PSS-coated multimode optical fiber was developed for the real-time monitoring of rabbit IgG detection. The developed biosensor contains TiO<sub>2</sub> nanoparticles on its surface, which enable the generation of LMRs, thanks to the high refractive index of this material in combination with PSS polymer, which can be activated physically. In this sense, a characterization of the immobilization and the detection process of this specific sensor will be described. This study also includes a comparison between two simple functionalization techniques based on the physical surface activation by both UV-ozone and plasma treatments. In addition, the reusability of the biosensor activated by plasma will be tested. Finally, some conclusions will be presented on the applicability of biosensing platforms based on TiO<sub>2</sub>/PSS thin films.

## II. METHODS AND MATERIALS

### A. Optical and Chemical Materials

Multimode optical fiber FT200EMT, with 200/225- $\mu$ m core/cladding diameter, was purchased from Thorlabs Inc., Bergkirchen, Germany, and UV optical adhesive from Norland Products Inc., East Windsor, NJ, USA. Titanium (IV) oxide (TiO<sub>2</sub>) nanoparticles of 21-nm-diameter, polymer PSS (Mw  $\sim$  70 000), phosphate buffered solution (PBS, 0.1 M) pH 7.2, bovine serum albumin (BSA), potassium hydroxide (KOH) 1 M, IgG from rabbit serum (essentially salt-free, lyophilized powder), and its specific polyclonal antibody antirabbit IgG produced in goat (lyophilized powder) were purchased from MERCK, Madrid, Spain. Both optical and chemical materials were used to fabricate the biosensors and to develop the bioassays.

### B. LMR Generation by Means of TiO<sub>2</sub>/PSS Thin Films

In the fabrication of the biosensor, first, the cladding of a 2-cm segment of the optical fiber was chemically removed and cleaned with acetone and acid piranha solution. Then, the LMR was obtained by coating the core exposed region with TiO<sub>2</sub>/PSS employing the LbL assembly technique, as explained in [10]. Briefly, the PSS water solution was used as the polyanionic solution, whereas the TiO<sub>2</sub> nanoparticles in ultrapure water were the cationic solution. The pH of both the polymer and the nanoparticle solutions was adjusted to 2.0. In each LbL cycle, the optical fiber was dipped for 2 min in the TiO<sub>2</sub> solution, washed out for 1 min in acid water, then dipped for 2 min in PSS solution, and finally washed out for 1 min in water (pH 2). These cycles were repeated to obtain the second LMR centered in a wavelength range from 600 to 750 nm, in order to track the wavelength shift of the LMR at every stage during the process.

### C. Instrumentation and Optical Setup

The transmission spectra were acquired using the optical setup and the microfluidic system detailed in Fig. 1(a). The

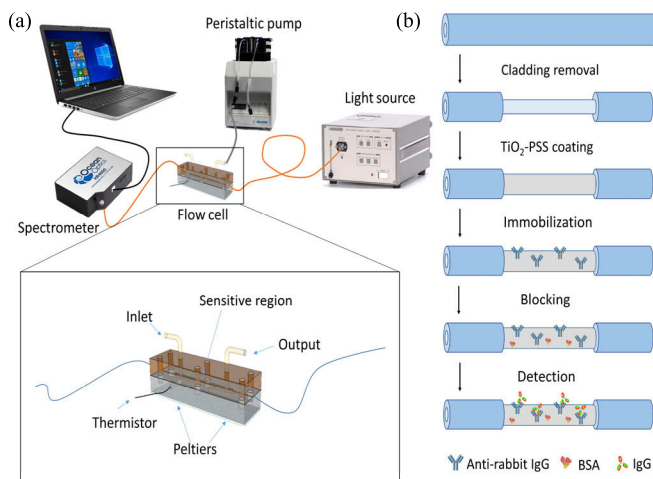


**Fig. 1.** (a) Complete experimental setup to check over in real time all the steps of the assay, the functionalization, and the detection of the rabbit IgG. The light goes through the optical fiber represented by an orange line from the light source to the spectrometer. The black line shows the cable that connects the spectrometer to the computer and collects the transmission spectral data. The inset shows the thermo-stabilized system in detail. (b) Sketch of the steps carried out to fabricate the proposed optical fiber biosensor.

sensitive region of the fiber was placed in the thermo-stabilized microfluidic system as described in [35]. Both ends of the fiber were connected to a halogen white light (Ando AQ-4303B) and to an HR4000 spectrometer (OceanInsight Inc., Ostfildern, Germany), respectively. The output wavelength range of the halogen white light was set to 400–1800 nm, and the HR4000 spectrometer allowed to measure in a range from 200 to 1100 nm. During the experimental assays, the transmission spectra data were sent from the spectrometer to the computer and were real time processed by Spectra Suite<sup>1</sup> (OceanInsight Inc., Ostfildern, Germany) and MATLAB<sup>1</sup> (The MathWorks, Inc., Natick, MA, USA) software.

As previously described in [35], the microfluidic system includes two equal-size parts (23 mm wide, 10 mm deep, and 100 mm long) made of polyetherimide (ULTEM resin) and stainless steel. A microchannel is fabricated on both the polyetherimide and in the stainless-steel parts, with the size of  $1 \times 1 \times 50$  mm, thus achieving a volume of  $50 \mu\text{L}$ . The size of the microchannel allows handling small fluid quantities. Two Peltier cells ( $23 \times 25$  mm) located below the stainless-steel part of the flow cell heat the system up, while a thermistor inside a lateral hole in the same stainless-steel part controls the temperature. Hence, the temperature during the experimental process is kept stable at  $30 \text{ }^\circ\text{C} \pm 0.05 \text{ }^\circ\text{C}$  by the thermostabilized microfluidic chamber. In addition, during the bioassays, the solutions are passed through the microfluidic cell with accurate flow rates, thanks to a peristaltic pump, which circulates the fluids using thermoplastic elastomer tubes.

#### D. Bioassay's Protocol

After the generation of an LMR with the TiO<sub>2</sub>/PSS thin film, the first step for the development of the biosensing assays was surface activation. Two different activation systems were tested, UV-ozone (Ossila Ltd, Sheffield, U.K.) and plasma (ACE1 Gala Instruments). The activation with UV-ozone required 30-min treatment, whereas the plasma

treatment needed just 5 min at 50 W. The fiber with its jacket was glued to the opposite ends of the flow cell system using the UV optical flexible adhesive indicated in Section II-A. After that, different solutions were pumped through it during the immobilization and detection process. As shown in Fig. 1(b), during the immobilization, the bioreceptor was attached to the surface and then the unreacted active functional groups were blocked. During the experiments, a solution of  $100 \mu\text{g/mL}$  of antirabbit IgG was flowed for an hour to attach the antibodies to the sensor surface. After that, PBS was flowed for 10 min, in order to rinse and remove the unbounded antibodies. The immobilization concluded by flowing during 10 min a blocking solution, BSA  $0.1 \text{ mg/mL}$  in PBS, and with a further PBS washing step. In the detection process, increasing concentrations of the analyte rabbit IgG were flowed for 20 min and the sensor surface was washed after each step with PBS until signal stabilization was achieved. The rabbit IgG-detected concentrations were 0.002, 0.02, 0.05, 0.2, 0.5, and 2 mg/mL diluted in PBS. All the steps of the experimental assays were performed at a flow rate of  $45 \mu\text{L/min}$ .

### III. RESULTS AND DISCUSSION

The biosensing platform is based on monitoring the LMR generated by the deposition of TiO<sub>2</sub>/PSS with the LbL method. The LMR wavelength shift is tracked in real time during every assay, allowing the detection and recording of the optical changes influencing the sensing layer behavior.

#### A. LMR Formation

As previously mentioned, the thin film is formed by depositing alternating layers of TiO<sub>2</sub> and PSS materials with washing steps in between. Fig. 2(a) shows the progress of the transmission peak, while the last bilayers of the coating are being deposited. The process is stopped when the second LMR is located between 600 and 750 nm. In addition, Fig. 2(b) presents a scanning electron microscope (SEM) image of the optical fiber coated by a TiO<sub>2</sub>/PSS thin film. As can be seen, the average thickness of the coating in the SEM measurements is estimated between 250 and 300 nm. These results are consistent with the theoretical and experimental results obtained by Del Villar et al. [36]. According to this, the obtained resonance corresponds to the second LMR, something that is confirmed by the 850-nm/Refractive Index Unit (RIU) sensitivity attained by the sensor in the refractive index range from 1.333 to 1.351 RIU (see Figs. S1 and S2 in the Supporting document).

It is important to emphasize that the optical fiber that has been used is standard  $200\text{-}\mu\text{m}$  multimode fiber. The use of a standard optical fiber as well as the position of the LMR in the visible instead of the infrared wavelength range reduces significantly the cost of the setup and brings it closer to commercialization.

#### B. Experimental Bioassays

During the experimental bioassays, the transmission spectrum is monitored in real time while the LMR wavelength shift is recorded. Fig. 3 shows the sensorgram of the LMR shift for a complete experimental bioassay. In this case, the optical fiber biosensor is previously activated with plasma. According to this, Fig. 3(a) and (b) represents the immobilization and detection process, respectively. The bioassay starts with the immobilization, which plays an important role concerning the development of the biosensors. In this section, the surface is

<sup>1</sup>Registered trademark.



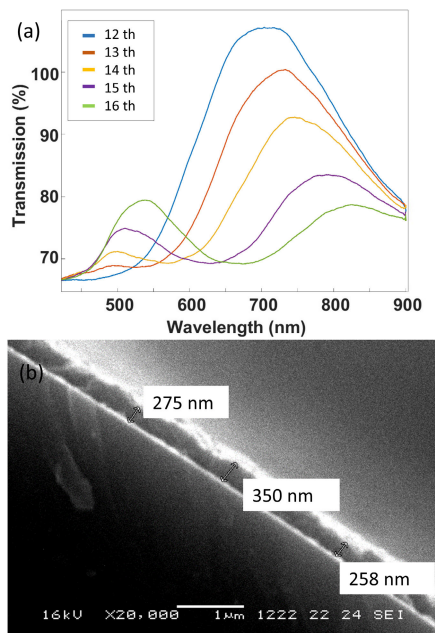


Fig. 2. (a) Experimental transmission spectra achieved in the last five layers of the  $\text{TiO}_2/\text{PSS}$  LbL deposition process. (b) SEM image of the optical fiber coated by the  $\text{TiO}_2/\text{PSS}$  layer.

covered with the antirabbit IgG bioreceptor. The antirabbit IgG is attached to the active groups of the PSS, obtaining a 13-nm wavelength shift. Then, the surface is rinsed with PBS as a way to remove the nonattached antirabbit IgG biomolecules. As it is noted in the sensorgram, the unreacted functional groups are blocked with BSA to avoid unspecific binding. The immobilization concludes with a new rinsing step in PBS.

The use of a specific bioreceptor for the analyte and the blocking of the surface permits the selective detection of rabbit IgG. The surface blocking prevents nonspecific interactions and interference, allowing the sensor to focus exclusively on the intended analyte. This selective approach enhances the accuracy and reliability of the detection process.

The sensorgram in Fig. 3(b) displays the signal change, compared to the baseline, of the rabbit IgG detection stage. During the detection, increasing concentrations of rabbit IgG are injected in a range between 0.002 and 2 mg/mL. After each analyte concentration, a washing step with PBS is carried out for the purpose of removing all the unbound rabbit IgG. The wavelength shift after the washing step corresponds to the amount of rabbit IgG bound to the specific bioreceptor and can be directly related to the increasing rabbit IgG concentration. The response of the sensor at the end of the washing steps remains stable, which demonstrates a consistent binding of the analyte.

### C. Plasma Versus UV-Ozone Activation Methods

Three complete independent bioassays ( $n = 3$ ) were developed with optical fibers activated by UV-ozone, and the other three complete independent bioassays ( $n = 3$ ) were developed after the functionalization with plasma treatment. The results obtained in the detection process after each activation treatment are shown in Fig. 4. The LMR wavelength shift is represented as a function of the rabbit IgG concentration. Here, it must be pointed out that the error bars correspond to the data of three independent biosensing assays ( $n = 3$ ), to assess the

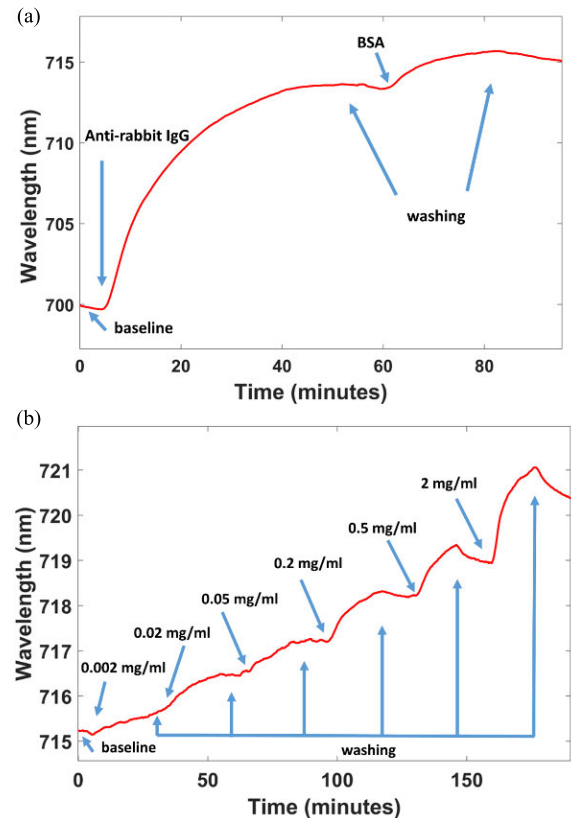


Fig. 3. (a) Sensorgram of the immobilization part of the experimental bioassays, comprising the antirabbit IgG attachment and the blocking step with BSA. (b) Sensorgram of the proposed biosensor during the detection of increasing rabbit IgG concentrations (range: 0.002–2 mg/mL).

repeatability of the present biosensor. The size of the error bars indicates certain variability on the data that can be attributed to different wavelength locations of the LMR in each experiment since it is well-known that it plays a role in the sensitivity of the LMR. In order to mitigate this problem, it will be necessary to control more precisely the parameters during the deposition of the LbL structure, i.e., pH of the solution, temperature, etc.

In Fig. 4, the experimental points are fit by the Hill function with an  $R^2$  regression coefficient of 0.9998 in the case of UV-ozone and 0.9989 in the case of plasma treatment. The Hill equation is a well-known mathematical model to quantify the degree of interaction between ligand binding sites [37]. Based on the recommendations made by the International Union of Pure and Applied Chemistry (IUPAC), it also permits to obtain the theoretical limit of detection (LOD) from the calibration curve of the biosensor. Specifically, the LOD is calculated as the average value of the blank signal plus three times the maximum standard deviation obtained among all the measurements, as reported in [38] and [39]. The theoretical LOD achieved from the UV-ozone treatment curve is 0.0195 mg/mL of rabbit IgG and 0.0312 mg/mL for the plasma treatment, which demonstrates that the results of both UV-ozone and plasma treatments are in the same order of magnitude.

According to these results, both UV-ozone and plasma functionalization systems are rapid and simple methods that are suitable for being used in optical fiber biosensor fabrication. UV-ozone functionalization takes 30 min, while plasma

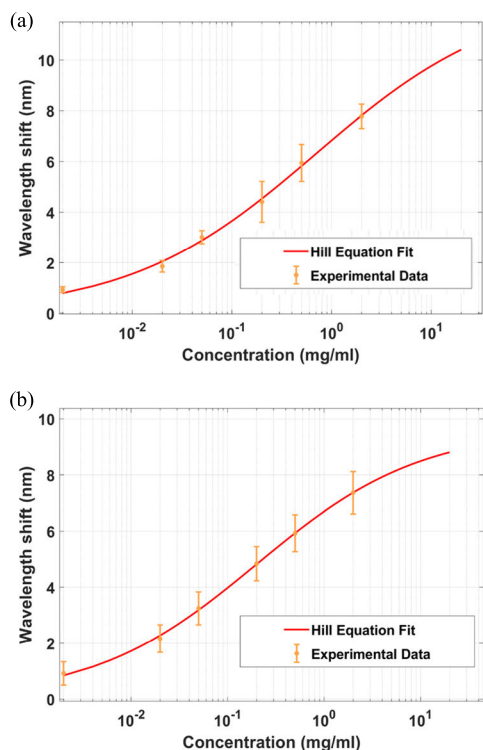


Fig. 4. Hill fitting curve of the experimental points obtained in the detection of different concentrations of rabbit IgG: (a) biosensors activated by plasma and (b) biosensors activated by UV-ozone. Both calibration curves are calculated from the results of three identical and independent biosensors ( $n = 3$ ). The error bars indicate the standard deviation of the experimental points for the three experiments.

treatment takes just 5 min, and then, the sensor is ready for the immobilization of the bioreceptor.

In contrast, as it is described in Table I, most of the functionalization methods present in the literature require more steps and longer processing times. Specifically, a functionalization based on a silanization process requires initial surface activation, silane attachment, drying, and silane group activation for bioreceptor attachment [18], [19], [20]. As an alternative, the functionalization technique based on an alkane thiol monolayer of mercaptoundecanoic acid (MUA) is frequently used for sensors based on gold thin films [17]. However, a longer period of time is needed for the adequate deposition of MUA onto the sensing surface, which is usually made overnight [21], [22], [23], [32], [33].

The next aspect to analyze is the sensitivity. It must be noted that other structures have already attained higher values than 850 nm/RIU, the sensitivity obtained by the proposed sensor. For instance, a sensor based on a single-mode optical fiber (SMF) core mismatch interferometer has presented a 14 000-nm/RIU sensitivity in [18]. In addition, the sensitivity attained with gold thin-film-coated photonic crystal fibers using gold nanoparticles is 3951 nm/RIU, something that has been overcome by using gold nanoparticles on an localized surface plasmon resonance (LSPR)-based sensor, reaching values between 2054 and 3980 nm/RIU [20].

However, in spite of being more sensitive, there is not a considerable difference achieved in the range of detected concentration among different strategies presented in Table I. The lowest detected concentration is attained using the described high-sensitivity interferometer [18]: 0.5 and 0.1  $\mu\text{g/mL}$  with

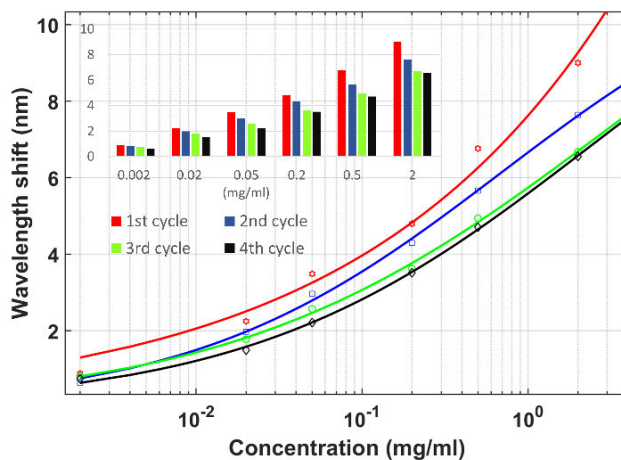


Fig. 5. Calibration curve of four experiments made in consecutive days with the same biosensor to test the reusability of the sensor. The fitting of the curves has been calculated by the Hill equation.

the nonreported sensitivity fiber bragg grating (FBG) sensor based on cladding mode resonance [20]. Those values are just an order of magnitude lower than 2  $\mu\text{g/mL}$ , reported as the lowest detected concentration in this work. The same minimum concentration has been achieved with a gold nanoparticle-based LSPR sensor (2  $\mu\text{g/mL}$ ) [33]. Even higher concentrations have been detected using an interferometric sensor constructed by a long thin-core single-mode fiber sandwiched between two SMFs (100–1000  $\mu\text{g/mL}$ ) [19] and a different LSPR sensor using nanorods (1–100  $\mu\text{g/mL}$ ) [23].

Given this, it is worth recognizing that the LOD parameters in the literature are excellent. According to Table I, the LOD reported with interferometers is 47 ng/mL [18], the lowest LOD for IgG detection with SPR is 37 ng/mL [40] and 0.8 nM (0.12  $\mu\text{g/mL}$ ) with gold nanorods-based LSPR sensor [33], while the lowest LOD is achieved with FBG based on cladding mode resonance coated with graphene oxide: 32 pM (4.8 ng/mL) [20]. The LOD reported in this work is 19.5  $\mu\text{g/mL}$  with plasma activation and 31.2  $\mu\text{g/mL}$  with UV-ozone activation. Contrary to most of the previous works here these values have been calculated from the calibration curve with the average value of three experiments, reflecting the deviation of the data among these three experiments.

Despite the previous considerations, there are undeniable advantages in favor of the presented functionalization in terms of reducing steps, which results in a consequent reduction of costs in both time and materials. In addition, given that the value of human IgG in normal adults relies within the range of 6–16  $\mu\text{g/mL}$  [34], the sensor proposed in this work has proven its useful value for the detection of IgG molecules.

Since the plasma treatment resulted in a shorter functionalization time and yielded comparable results, the reusability of these sensors was tested using the plasma treatment.

#### D. Reusability

The physical and chemical resistances of TiO<sub>2</sub>/PSS coating make it an ideal material to create reusable biosensors. In this study, the position of the LMRs has been checked during all the experimental period. In this sense, the transmission spectrum of the fiber employed during the experiment in Fig. 3 was registered after a year and it was included in Fig. S3 of the supporting document. In the same document, Fig. S4 shows

**TABLE I**  
COMPARATIVE ANALYSIS OF DIFFERENT OPTICAL FIBER SENSORS EMPLOYED FOR THE DETECTION OF IGG BIOMOLECULES

Sensor configuration	Transduction method	Functionalization		Activation		Sensitivity (nm/RIU)	LOD	Concentration range	Ref.
		Technique	Time	System	Time				
SMF (core mismatch)	Mach Zehnder interferometer	Piranha + APTES	1 h + 1 h	Glutaraldehyde + Protein A	2 h 1 h	-14,000	47 ng/ml	0.5 - 50 µg/ml	[18]
SMF - thin core - SMF	Mach Zehnder interferometer	Piranha + APTES	30 min + 24 h	Glutaraldehyde	1 h	82.7	-	100 - 1000 µg/ml	[19]
Au film coated PCF + AuNPs	SPR + LSPR	MUA	12 h	EDC + NHS + Protein A	20 min 1 h	3,915	37 ng/ml	1 - 30 µg/ml	[32]
SMF- PMF - SMF + Au film	SPR	MUA	12 h	EDC + NHS	30 min	1,625	3.4 µg/ml	10 - 100 µg/ml	[21]
SPR image sensor	SPR	MUA	overnight	EDC + NHS	15 min	-	47.4 nM (7.1 µg/ml)	67 nM - 1 µM (10-150 µg/ml)	[22]
LSPR (AuNPs)	LSPR	PDA	30 min	EDC + NHS	30 min	2,054	2 µg/ml	2 - 100 µg/ml	[23]
		MUA	12 h			3,980	6.02 µg/ml	10 - 100 µg/ml	
LSPR (Au nanorods)	LSPR	MUA	12 h	EDC + NHS	15 min	753	0.8 nM (0.12 µg/ml)	6.7 - 667 nM (1-100 µg/ml)	[33]
FBG based on cladding mode resonance (/GO coating)	FBG	Piranha + APTES	30 min + 30 min	Glutaraldehyde	30 min	-	306 pM (46 ng/ml)	0.667 nM - 670 nM (0.1 - 100 µg/ml)	[20]
		Piranha + APTES + GO	30 min + 30 min + overnight	EDC + NHS	20 min	-	32 pM (4.8 ng/ml)		
LMR TiO <sub>2</sub> /PSS	LMR	-	-	Plasma	5 min	850	19.5 µg/ml	2 - 200 µg/ml	This work
				UV-ozone	30 min		31.2 µg/ml		

A vertical slash (/) indicates that the article compares the results obtained by two different sensors, with different functionalizations.

the results of the experimental bioassay developed a year after the fabrication of the LMR.

In addition, the reusability of an individual biosensor was analyzed in Fig. 5 by performing the complete bioassays for four consecutive days using the same LMR. The calibration curves are obtained with the Hill equation. The value of the  $R^2$  regression coefficient exceeds 0.99 in all cases. As noted in Fig. 5, even if the sensitivity of the biosensor decreases in each cycle of detection, it still detects all the concentrations of the target molecule after four cycles. As an example, the highest concentration, 2 mg/mL, leads to a 9-nm wavelength shift in the first cycle, 7.64 nm in the second cycle, 6.68 nm in the third cycle, and 6.56 nm in the last cycle. In terms of percentages, this means a reduction of 15.8% between the first and second cycles, 10.7% between the second and third cycles, and just 1.3% between the third and fourth cycles. After four cycles, the biosensor keeps 72.9% of the initial detection capacity, as can be observed in the inset of Fig. 5.

#### IV. CONCLUSION

In this work, an easy-to-handle, fast, and robust real-time LMR biosensor has been developed based on the properties of the TiO<sub>2</sub>/PSS coating. The TiO<sub>2</sub>/PSS LMR is generated by the well-known LbL technique. Once the LMR is generated, the optical fiber is functionalized by either UV-ozone or plasma treatments. After that, the effectiveness of both plasma and ozone activation methods for the functionalization of the PSS was verified.

One of the characteristic highlights of the proposed biosensor is that it requires a short and easy functionalization protocol for the bioreceptor attachment, which is based on a physical activation of the TiO<sub>2</sub>/PSS coating. This promotes the direct attachment of the rabbit IgG to the sensing layer surface. After that, the biosensor allows the specific and label-free detection of biomolecules. In this case, a concentration range from 0.002 to 2 mg/mL of rabbit IgG can be successfully detected. In addition, due to the chemical and physical resistance of the TiO<sub>2</sub>/PSS coating, the biosensor

presents a stable time response and reusability for at least four consecutive cycles. After the detection of rabbit IgG, a plasma activation cycle is enough to restart a complete bioassay.

The real-time detection, as well as label-free capabilities, entails a noticeable departure from the current methodology and significant cost reduction. Less time is necessary to obtain results and fewer materials are required. Furthermore, the ability to perform these detections in the visible spectrum, although reducing sensitivity, enables the use of simpler and more affordable optical equipment, thus paving the way for potential future commercialization.

Additionally, the functionalization proposed in this study could also be applied to other more sensitive optical structures and materials to achieve the detection of smaller biomolecules or molecules with a more demanding LOD.

#### REFERENCES

- [1] X. D. Wang and O. S. Wolfbeis, "Fiber-optic chemical sensors and biosensors (2013–2015)," *Anal. Chem.*, vol. 88, no. 1, pp. 203–227, 2016.
- [2] A. B. Socorro-Leránoz, D. Santano, I. Del Villar, and I. R. Matias, "Trends in the design of wavelength-based optical fibre biosensors (2008–2018)," *Biosensors Bioelectronics*, X, vol. 1, Jun. 2019, Art. no. 100015.
- [3] N. Jiang et al., "Functionalized flexible soft polymer optical fibers for laser photomedicine," *Adv. Opt. Mater.*, vol. 6, no. 3, pp. 1–10, Feb. 2018.
- [4] C. Chen and J. Wang, "Optical biosensors: An exhaustive and comprehensive review," *Analyst*, vol. 145, no. 5, pp. 1605–1628, 2020.
- [5] B. Carotenuto et al., "Smart optical catheters for epidurals," *Sensors*, vol. 18, no. 7, p. 2101, 2018.
- [6] G. Cheymol, B. Brichard, and J. F. Villard, "Fiber optics for metrology in nuclear research reactors—Applications to dimensional measurements," *IEEE Trans. Nucl. Sci.*, vol. 58, no. 4, pp. 1895–1902, Aug. 2011.
- [7] I. Dominguez et al., "Spectral measurements with hybrid LMR and SAW platform for dual parameter sensing," *Analyst*, vol. 147, no. 23, pp. 5477–5485, 2022.
- [8] I. Del Villar et al., "Optical sensors based on lossy-mode resonances," *Sens. Actuators B, Chem.*, vol. 240, pp. 174–185, Mar. 2017.
- [9] S. P. Usha, A. M. Shrivastav, and B. D. Gupta, "Semiconductor metal oxide/polymer based fiber optic lossy mode resonance sensors: A contemporary study," *Opt. Fiber Technol.*, vol. 45, pp. 146–166, Nov. 2018.



- [10] M. Hernaez, I. D. Villar, C. R. Zamarreno, F. J. Arregui, and I. R. Matias, "Optical fiber refractometers based on lossy mode resonances supported by TiO<sub>2</sub> coatings," *Appl. Opt.*, vol. 49, no. 20, pp. 3980–3985, 2010.
- [11] M. Geetha, A. K. Singh, R. Asokamani, and A. K. Gogia, "Ti based biomaterials, the ultimate choice for orthopaedic implants—A review," *Prog. Mater. Sci.*, vol. 54, no. 3, pp. 397–425, May 2009.
- [12] M. Kulkarni et al., "Protein interactions with layers of TiO<sub>2</sub> nanotube and nanopore arrays: Morphology and surface charge influence," *Acta Biomaterialia*, vol. 45, pp. 357–366, Nov. 2016.
- [13] S. Jafari, B. Mahyad, H. Hashemzadeh, S. Janfaza, T. Gholikhani, and L. Tayebi, "Biomedical applications of TiO<sub>2</sub> nanostructures: Recent advances," *Int. J. Nanomedicine*, vol. 15, pp. 3447–3470, May 2020.
- [14] R. Adzhri et al., "Reactive Ion etching of TiO<sub>2</sub> thin-film: The impact of different gaseous," in *Proc. IEEE Regional Symp. Micro Nanoelectronics*, Aug. 2015, pp. 8–11.
- [15] T. Bhardwaj, "Review on biosensor technologies," *Int. J. Adv. Res. Eng. Technol.*, vol. 1962, pp. 36–62, Feb. 2015.
- [16] B. I. Karawdeniya et al., "Surface functionalization and texturing of optical metasurfaces for sensing applications," *Chem. Rev.*, vol. 122, no. 19, pp. 14990–15030, Oct. 2022.
- [17] N. Sandhyarani, *Surface Modification Methods for Electrochemical Biosensors*. Amsterdam, The Netherlands: Elsevier, 2019.
- [18] B.-T. Wang and Q. Wang, "An interferometric optical fiber biosensor with high sensitivity for IgG/anti-IgG immunosensing," *Opt. Commun.*, vol. 426, pp. 388–394, Nov. 2018.
- [19] Y. Zheng, T. Lang, T. Shen, and C. Shen, "Simple immunoglobulin G sensor based on thin core single-mode fiber," *Opt. Fiber Technol.*, vol. 41, pp. 104–108, Mar. 2018.
- [20] S. Chen et al., "A fiber Bragg grating sensor based on cladding mode resonance for label-free biosensing," *Biosensors*, vol. 13, no. 1, p. 97, Jan. 2023.
- [21] Y. Huang et al., "Compact surface plasmon resonance IgG sensor based on H-shaped optical fiber," *Biosensors*, vol. 12, no. 3, p. 141, 2022.
- [22] Y. Liu, Q. Liu, S. Chen, F. Cheng, H. Wang, and W. Peng, "Surface plasmon resonance biosensor based on smart phone platforms," *Sci. Rep.*, vol. 5, no. 1, pp. 1–9, Aug. 2015.
- [23] S. Shi et al., "A polydopamine-modified optical fiber SPR biosensor using electroless-plated gold films for immunoassays," *Biosensors Bioelectron.*, vol. 74, pp. 454–460, Dec. 2015.
- [24] F. Chiavaioli et al., "Femtomolar detection by nanocoated fiber label-free biosensors," *ACS Sensors*, vol. 3, no. 5, pp. 936–943, May 2018.
- [25] G. Nageswaran, L. Jothi, and S. Jagannathan, *Plasma Assisted Polymer Modifications*. Amsterdam, The Netherlands: Elsevier, 2018.
- [26] A. Bhattacharyya and C. M. Klapperich, "Mechanical and chemical analysis of plasma and ultraviolet–ozone surface treatments for thermal bonding of polymeric microfluidic devices," *Lab Chip*, vol. 7, no. 7, pp. 876–882, 2007.
- [27] J.-P. Booth, M. Mozetic, A. Nikiforov, and C. Oehr, "Foundations of plasma surface functionalization of polymers for industrial and biological applications," *Plasma Sources Sci. Technol.*, vol. 31, no. 10, Oct. 2022, Art. no. 103001.
- [28] C. Alemán, G. Fabregat, E. Armelin, J. J. Buendía, and J. Llorca, "Plasma surface modification of polymers for sensor applications," *J. Mater. Chem. B*, vol. 6, no. 41, pp. 6515–6533, 2018.
- [29] A. N. Yusilawati et al., "Surface modification of polystyrene beads by ultraviolet/ozone treatment and its effect on gelatin coating," *Amer. J. Appl. Sci.*, vol. 7, no. 6, pp. 724–731, 2010.
- [30] H. Liu et al., "Temperature-insensitive label-free sensors for human IgG based on S-tapered optical fiber sensors," *IEEE Access*, vol. 9, pp. 116286–116293, 2021.
- [31] S. Agarwal and C. Cunningham-Rundles, "Assessment and clinical interpretation of reduced IgG values," *Ann. Allergy, Asthma Immunol.*, vol. 99, no. 3, pp. 281–283, Sep. 2007.
- [32] B.-T. Wang and Q. Wang, "Sensitivity-enhanced optical fiber biosensor based on coupling effect between SPR and LSPR," *IEEE Sensors J.*, vol. 18, no. 20, pp. 8303–8310, Oct. 2018.
- [33] M. Lu, H. Zhu, L. Hong, J. Zhao, J.-F. Masson, and W. Peng, "Wavelength-tunable optical fiber localized surface plasmon resonance biosensor via a diblock copolymer-templated nanorod monolayer," *ACS Appl. Mater. Interfaces*, vol. 12, no. 45, pp. 50929–50940, Nov. 2020.
- [34] P. J. Worsfold, A. Hughes, and D. J. Mowthorpe, "Determination of human serum immunoglobulin G using flow injection analysis with rate turbidimetric detection," *Analyst*, vol. 110, no. 11, pp. 1303–1305, 1985.
- [35] F. Chiavaioli et al., "Towards sensitive label-free immunosensing by means of turn-around point long period fiber gratings," *Biosensors Bioelectron.*, vol. 60, pp. 305–310, Oct. 2014.
- [36] I. Del Villar et al., "Design rules for lossy mode resonance based sensors," *Appl. Opt.*, vol. 51, no. 19, pp. 4298–4307, Jul. 2012.
- [37] B. I. Kurganov, A. V. Lobanov, I. A. Borisov, and A. N. Reshetilov, "Criterion for Hill equation validity for description of biosensor calibration curves," *Analytica Chim. Acta*, vol. 427, no. 1, pp. 11–19, Jan. 2001.
- [38] G. L. Long and J. D. Winefordner, "Limit of detection. A closer look at the IUPAC definition," *Anal. Chem.*, vol. 55, no. 7, pp. 712–724, Jun. 1983.
- [39] A. Shrivastava and V. Gupta, "Methods for the determination of limit of detection and limit of quantitation of the analytical methods," *Chronicles Young Scientists*, vol. 2, no. 1, p. 21, 2011.
- [40] S. Saekow, W. Maiakgree, W. Jarernboon, S. Pimanpang, and V. Amornkitbamrung, "High intensity UV radiation ozone treatment of nanocrystalline TiO<sub>2</sub> layers for high efficiency of dye-sensitized solar cells," *J. Non-Crystalline Solids*, vol. 358, no. 17, pp. 2496–2500, Sep. 2012.



**Desiree Santano Rivero** received the M.Sc. degree in microbiology and health from the University of the Basque Country (UPV/EHU), Bilbao, Spain. She is currently pursuing the Ph.D. degree with the Public University of Navarra (PUN-UPNA), Pamplona, Spain.

She has been a Biologist (UPV/EHU) since 2013. She has coauthored communications related to microbiology and biomedical engineering. Her research interests focus on the biomedical engineering field, including the development of optical fiber biosensors.



**Abián B. Socorro-Leránóz** received the degree in telecommunications engineering, the M.Sc. degree in biomedical engineering, and the Ph.D. degree in engineering from the Public University of Navarra (PUN-UPNA), Pamplona, Navarra, Spain, in 2010, 2012, and 2015, respectively.

He joined the Armani Research Laboratory, University of Southern California, Los Angeles, CA, USA, as a Visiting Ph.D. Student, in 2014. He is currently working as an Associate Professor with PUN-UPNA, where he has authored

80 scientific contributions both in JCR journals and conferences and he has been involved in more than 20 competitive research projects with both public and private funding. His research interests are the development of photonic sensors (optical fiber sensors mainly), including biosensors and, in general, the development of biomedical applications based on photonics.



**Ignacio Del Villar** (Member, IEEE) received the M.S. degree in electrical and electronic engineering and the Ph.D. degree from the Public University of Navarra, Pamplona, Navarra, Spain, in 2002 and 2006, respectively, with a specialty in optical fiber sensors.

He has been an Associate Professor with UPNA since 2021. His research interests include optical fiber sensors and the effect of nanostructured coatings deposited on waveguides.